MedChemComm

Accepted Manuscript

ROYAL SOCIETY OF CHEMISTRY

www.rsc.org/medchemcomm

Multivalent Amino Sugars to Recognize Different TAR RNA Conformations†

Patrick C. Kellish[a], Sunil Kumar[a], Todd S. Mack[c], Meredith Newby Spano[b], Mirko Hennig[c] and Dev P. Arya[a,b*]

[a]Laboratory of Medicinal Chemistry, Department of Chemistry, Clemson University, Clemson, South Carolina 29634, United States

[b]NUBAD, LLC, 900B West Faris Rd., Greenville, SC 29605

[c]Department of Biochemistry and Molecular Biology, Medical University of South Carolina, 70 President St., Charleston, SC 29425

* To whom correspondence should be addressed: Dev P Arya, 461 H.L. Hunter Chemistry Labs, Department of Chemistry, Clemson University, Clemson University, Clemson, South Carolina 29634; Phone: +1-864-656-1106; Fax: +1-864-656-6613; E-mail: dparya@clemson.edu.

†Electronic Supplementary Information (ESI) available: [Chemical structures of all compounds studied, CD spectroscopic characterization, UV thermal denaturation, ethidium bromide displacement assays and NMR characterizations].

ABSTRACT
Neomycin dimers synthesized using "click chemistry" with varying functionality and length in the linker region have been shown to be effective in targeting the HIV-1 TAR RNA region of the HIV virus. TAR (Transactivation Response) RNA region, a 59 base pair stem loop structure located at the 5'-end of all nascent viral transcripts interacts with its target, a key regulatory protein, Tat, and necessitates the replication of HIV-1 virus. Ethidium bromide displacement and FRET competition assays have revealed nanomolar binding affinity between neomycin dimers and wildtype TAR RNA while in case of neomycin, only a weak binding was detected. Here, NMR and FID-based comparisons reveal an extended binding interface for neomycin dimers involving the upper stem of the TAR RNA thereby offering an explanation for increased affinities. To further explore the potential of these modified aminosugars we have extended binding studies to include four TAR RNA mutants that display conformational differences with minimal sequence variation. The differences in binding between neomycin and neomycin dimers is characterized with TAR RNA mutants that include mutations to the bulge region, hairpin region, and both the bulge and hairpin regions. Our results demonstrate the effect of these mutations on neomycin binding and our results show that linker functionalities between dimeric units of neomycin can distinguish between the conformational differences of mutant TAR RNA structures.

Introduction

Ribonucleic acid-protein interactions are essential for the regulation of many important biological processes such as translation, RNA splicing and transcription[1-3]An important example of such an interaction is involved in the regulation of human immunodeficiency virus type 1 (HIV-1). TAR RNA (trans activation responsive region), a 59 base stem-loop structure located at the 5'-end of the nascent viral transcripts that interacts with Tat protein (an 86 amino acid protein) and regulates the transcription level of HIV[4, 5]. The cooperative interaction of Tat protein along with its cellular cofactor, transactivating elongation factor-b (TEFb) with TAR RNA recruits and activates the CDK9 kinase which phosphorylates the RNA polymerase II (RNAP II) and significantly enhances the processivity of RNAP II [3, 6, 7]. HIV transcription in virus-infected cells is strongly triggered by the interaction between Tat protein and its cognate TAR RNA. Because of the key role played by the TAR RNA in HIV-1 viral proliferation, the structure and dynamics of this RNA stem-loop has been studied extensively[8]. TAR RNA structure is comprised of two stems (upper and lower), a three nucleotide bulge region, and a hairpin. The upper stem and lower stems move relative to one another, bending at the tri-nucleotide bulge loop "joint" (U23, C24, and U25), sampling many conformations in solution[9]. An arginine-rich domain of Tat protein interacts with the tri-nucleotide bulge of TAR RNA [1, 10, 11], attenuating the motion of the TAR stem-loop and causing a substantial enhancement in the viral transcript level (~100 fold) [2]. The amenable size, modular nature, and biological and medical import of the TAR RNA stem-loop has made it a popular target for ligand binding studies in recent years.

Given the ubiquity of RNA-mediated biological processes, molecules that can selectivity bind and regulate the function of RNA have enormous potential for applications in biotechnology and therapeutics [12]. Although considerable effort in utilizing RNA as a drug target, discovery of molecules with desirable drug-like properties remains challenging and is the focus of intense investigation [13]. RNA is often characterized by a variety of secondary structures including, hairpins, bulges, stems, loops, pseudo-knots, and turns [12]. Folding of these local secondary

structural elements gives rise to unique tertiary structures unique to RNA, providing the potential for RNA to be targeted specifically [14].

Targeting these three-dimensional RNA structures by small molecules has been well demonstrated by rRNA binding to aminoglycosides, macrolide, oxazolidinone, and tetracycline antibiotics [15-20]. In addition this approach has been extended to the disruption of TAR-Tat interactions with small molecules[13] including intercalators[21] (ethidium bromide and proflavine), DNA minor groove binders[22] (Hoechst 33258 and DAPI), phenothiazine[23], argininamide[24], peptides[25], peptidomimetics[26], aminoglycosides[27, 28], and cyclic polypeptides[29]. Aminoglycosides are naturally occurring amino sugars that bind a variety of RNA structures [16]. In the past few years, a number of aminoglycoside conjugates have been synthesized to achieve higher binding affinity and specificity towards RNA-[16, 30-34] and DNA-based targets[35-52], such as duplex[53], triplex[54-56], and quadruplex structures[37, 38]. Aminoglycoside binding to TAR RNA has previously been shown to be more than a simple electrostatic attraction via of ammonium groups; for example, streptomycin (+3 charge) is 10-fold less effective than neomycin (six amino groups) but is about 5-fold more effective than the more cationic gentamicin (+5 charge) in inhibiting Tat binding[57]. This data supports the notion that neomycin displays a conformational preference for certain RNA structures, such that the placement of some of these amino groups is more important that the total number of such groups. However, small molecules such as neomycin have been subject to selectivity issues[13, 24, 25, 27, 58-60]. We have previously detailed the binding of neomycin conjugates including neomycin dimers, synthesized using click chemistry, to wildtype TAR RNA[28, 61]. In addressing the selectivity issues and further expanding the potential of modified amino sugars, we report the selectivity of neomycin dimers synthesized using click chemistry with different linker functionalities to four TAR RNA mutants (figure 1) with different conformations. These constructs were designed with the intent to eventually distinguish between ligand interactions with the various TAR RNA binding domains: the tri-nucleotide bulge, the hairpin loop, and the helical stem regions, versus another. Our results show that the mutant TAR RNAs adopt different conformations, and there is differential binding of these TAR RNA conformations based on linker functionality and length of the neomycin dimers. In addition, the dependence of neomycin's specificity to different RNA conformations is also investigated. These findings further expand the potential of modified amino sugars in the recognition and specificity of biologically relevant RNA conformations.

Results and Discussion

CD Spectroscopy Studies for Characterizing Wildtype and Mutant TAR RNA Conformational Differences

CD spectroscopy has been shown to be a powerful tool for monitoring and characterizing the binding interactions between macromolecules (nucleic acids and proteins) and ligands[40, 41]. CD spectroscopy can provide useful insight into the comparative change in the conformation of the macromolecule [40]. In addition, identifying conformational differences between target macromolecules can be accomplished through the use of CD spectroscopy.

The CD spectrum of wildtype TAR RNA features a strong positive peak at 265 nm and a strong negative peak at 210 nm. In addition, there is a negative peak observed at ~240 nm, and is indicative of an A-form RNA conformation. Previous CD studies of the Tat/TAR RNA complex

revealed a substantial change in the structure of wildtype TAR RNA induced by the Tat protein. During the Tat-TAR RNA binding interaction there is a slight redshift observed at 265 nm. Additionally, the CD intensity of TAR RNA at 265 nm decreases by 15%[62]. The positive CD peak at 265 nm is a signature peak for the tri-nucleotide bulge region (UCU) and has been attributed to the arrangement of base stacking in the bulge region[30]. During the Tat-TAR RNA interaction, the Tat protein binds at its primary binding site, which is the tri-nucleotide bulge region, and modifies the arrangement of base stacking in the bulge region. The binding interaction was monitored by a decrease in the CD intensity at 265 nm. In addition, there is a marginal redshift observed at 265 nm, indicative of the small distortion of bulge structure.

CD titrations of neomycin into TAR RNA have demonstrated that neomycin induces a change in TAR RNA conformation upon binding that is distinct from the conformational changes induced by the Tat protein[30]. Previously we have reported neomycin dimers cause a gradual increase in CD intensity of the negative peak at 210 nm and 240 nm, with no change in CD intensity to the positive peak at 265 nm, only observing a slight redshift in this region[28]. The functionality of the neomycin dimer linker region (figure 2) also plays a role in the structural changes induced upon binding to wildtype TAR RNA. To illustrate how linker functionality influences structural changes we examined the changes seen with two neomycin dimers having equal linker length but different functionalities, DPA51 and DPA65 with wildtype TAR RNA. Surprisingly, the neomycin dimers DPA51 and DPA65 had different effects on the conformation of wildtype TAR RNA. To better compare these regions of conformational change, we plotted the change in the wildtype TAR RNA CD spectra (ΔCD) induced by neomycin dimers DPA51 and DPA65 (figure 3). The changes seen in the 210-220 nm region were the same for both DPA51 and DPA65. Interestingly, the changes seen in the 225-300 nm range were different for DPA51and DPA65. Most notably DPA65 showed no redshift, but showed increased intensity in the 265 nm region; these findings were not seen with DPA51, the Tat protein, or neomycin[28, 62, 63]. Therefore, we show that neomycin dimers can bind the Tat protein binding site of wildtype TAR RNA and depending on the linker functionality alter the conformation differently than observed from the TAR-Tat interaction. This finding reveals the possibility that differences in neomycin dimer linkers could show selectivity for different conformations of TAR RNA.

To further explore the recognition of TAR RNA conformations by neomycin dimers, CD spectroscopy was employed to detect any conformational deviations of four TAR RNA mutants from the wildtype TAR RNA conformation (figure 4). In addition, the conformational changes induced by neomycin dimer DPA51 were compared with all TAR RNA constructs (figure 5 and 6). Comparisons of each TAR RNA mutant to wildtype TAR RNA CD spectra revealed that each TAR RNA mutant adopts a conformation that has different local and/or global architectural features than that of the wildtype TAR RNA.

The conformational effect of the TAR RNA mutations is not limited to the region that is associated with the tri-nucleotide bulge, except in the case of the U3 bulge mutant. The U3 bulge mutant, which has a single base pair substitution in the bulge region (C to U), showed a deviation from wildtype TAR RNA conformation in the spectral region associated with the tri-nucleotide bulge. This decrease in CD intensity of the positive 265 nm peak of about 25% is similar to the change in CD signal intensity observed upon Tat binding to wildtype TAR, although interestingly, the single base substitution has a more pronounced effect on base stacking.

Complete removal of the bulge region of TAR RNA showed both a decrease in CD intensity in the positive 265 nm peak and an increase in CD intensity of the negative peak at 210 nm.

Conformational effects of TAR RNA not only arise from alterations in the bulge region, as mutations in the loop region are also observed to alter the RNA structure. Evidence of this fact is shown with the tetraloop TAR RNA mutant, in which a two base deletion in the loop region results in a four base loop. The tetraloop TAR RNA mutant displayed a decrease in CD intensity in the positive 265 nm peak of ~15%, similar to the change observed upon Tat protein binding, although the decrease in CD intensity in this region is accompanied with a slight redshift not seen with Tat protein binding. In addition, the negative peak at 210 nm of the tetraloop TAR RNA mutant displayed a decrease in CD intensity of ~25% but lacked the distinctive red shift observed for the 265 nm peak.

When the bulgeless and tetraloop mutations are compounded, the conformational effects differ from those observed for the bulgeless and tetraloop mutantations alone. The bulgeless tetraloop TAR RNA mutant's negative peak at 210 increased in CD intensity, similar to the effect seen by the bulgeless TAR RNA mutant. The positive peak at 265 nm the bulgeless tetraloop TAR RNA mutant showed a decrease in CD intensity similar to the degree of change observed for the tetraloop TAR RNA mutant, but lacked the redshift observed with the tetraloop TAR RNA mutant.

The effect of neomycin dimers on the conformation of the TAR RNA mutants was examined with neomycin dimer DPA51 (figure 5 and 6). Neomycin dimer DPA51 induced a redshift in all TAR RNA mutants. Although a slight redshift was observed with DPA51 and wildtype TAR RNA this redshift effect is much greater with the TAR RNA mutants. In the presence of DPA51 all TAR RNA mutants showed an increase in CD intensity in the 260-270 nm range that was greater than observed with wildtype TAR RNA. Interestingly, removal of the bulge region resulted in greater intensity increases in the 260-270 nm range. All the TAR RNA mutants showed less change in the 210-220 nm range compared to wildtype TAR RNA except the U3 bulge TAR RNA, which displayed the same degree of change in this range as wildtype TAR. Although the TAR RNA mutants adopt a different conformations, we show how neomycin dimers can induce unique conformational changes in each TAR RNA mutant that are distinctly different than the changes seen with wildtype TAR RNA.

The ability to detect such differences in CD spectra between the wildtype and mutant TAR RNA structures clearly suggests that these TAR RNA mutants adopt distinctly different conformations than wildtype TAR RNA, at least locally at the mutated bulge and loop regions of the TAR RNA. However, it has been observed that small alterations in the TAR bulge sequence may alter the global conformation and dynamics of the molecule. For example, studies by Al-Hashimi and co-workers have shown that altering the identity of TAR bulge nucleotides results in drastic changes in the angle between the two helical stem-loops as well as the dynamics between them[64]. Importantly, the conformational differences between wildtype TAR RNA and TAR RNA mutants and the finding that neomycin dimers induce conformational changes in the TAR RNA mutants provides an excellent platform to investigate the structure-activity relationship of modified amino sugar nucleic acid-binding ligands. Further characterization of the neomycin dimers with the various TAR RNA mutants will reveal the differences in the linker region

between the neomycin units (figure 2) that contribute to selectivity of these different RNA structures (figure 1).

Influence of Neomycin and Neomycin Dimers on Thermal Stability of TAR RNA Conformations

Thermal stability has been an effective measure to study the interaction of the Tat protein- and TAR RNA-binding ligands. Tat protein-induced thermal stability was observed to be salt dependent, with a 8.5 ^{o}C increase in T_m at 20 mM Na^+ but only a 3.0 ^{o}C T_m increase at 80 mM Na^+ [62]. In addition, we have previously reported the ability of neomycin dimers to induce thermal stability of wildtype TAR RNA, increasing the T_m from 3.3-10.2 ^{o}C at 100 mM salt concentrations. The ability of neomycin dimers to induce thermal stability of wildtype TAR RNA decreases with increasing the linker length between the neomycin subunits. Neomycin was shown to induce very little thermal stability in wildtype TAR RNA, increasing the T_m by 0.2 ^{o}C [28].

To explore the interactions between neomycin and neomycin dimers with TAR RNA mutants, UV thermal denaturation were conducted to determine both the effect of the TAR RNA mutations on the thermal denaturation, and if neomycin or neomycin dimers induce thermal stability (figure 7). UV thermal denaturation studies were conducted with the TAR RNA mutants in the absence of ligand, with one equivalent of the neomycin dimer DPA51, 1 equivalent neomycin, and 2 equivalents neomycin.

Results from the UV thermal denaturation experiments of the TAR RNA mutants in the absence of ligand revealed that the mutations to TAR RNA alter its thermal stability (Table 1). Removal of the bulge region of TAR RNA had the most influence of all the mutations on increasing the thermal stability. These observations provide evidence that the bulge region of TAR RNA alone greatly decreases the thermal stability. Interestingly, we observe a marked increase in melting temperature with the U3 mutant, as compared with wildtype TAR. Also worth noting is that the melting temperature for the bulgeless tetraloop is only slightly higher (by three degrees Celsius) than that of the bulgeless TAR.

Neomycin dimer DPA51 was observed to increase the thermal stability of all TAR RNA mutants, but to a lesser degree than the increase in thermal stability observed with wildtype TAR RNA (Table 1). Neomycin conferred very little increase in thermal stability for all TAR RNA mutants at one and two equivalents, which is consistent with the observations of neomycin with wildtype TAR RNA. Taken together, the thermal denaturation studies show that while the TAR RNA mutants display differences in thermal stability in the absence of ligand, neomycin dimers increase the thermal stability of all mutants, but to a lesser extent than observed for wildtype TAR RNA. In addition, neomycin monomer at one and two equivalents only confers very little increase in thermal stability, a similar observation observed for wildtype TAR RNA.

Ethidium Bromide Displacement Assay for Characterizing the Binding of Neomycin and Neomycin to Wildtype and Mutant TAR RNA Conformations

To further investigate the binding between neomycin and neomycin dimers, ethidium bromide displacement assays were performed. The affinities of neomycin dimers were observed to be directly proportional to the amount of ethidium bromide displaced from TAR RNA, and are reflected in the IC_{50} values (concentration of ligand required to displace 50% ethidium bromide) (Table 2). The displacement of ethidium bromide as a function of neomycin dimer concentration results in a saturating binding plot from which the binding stoichiometry may be deduced (Figure 8). Since neomycin dimers have been shown to have a binding stoichiometry of 1:1 with wildtype TAR RNA, the ethidium bromide displacement titrations were used to obtain the association constant using Scatchard analysis (Figure 8) [65]. The slope of this plot allows for the determination of the association constants with the TAR RNA mutants (Table 3).

The affinities of neomycin for the TAR RNA mutants maintaining the bulge region were lower than for the wildtype TAR RNA, although removal of the bulge region resulted in an increase of neomycin affinity. Surprisingly, TAR RNA mutants lacking the bulge region bind both neomycin and neomycin dimers with a stoichiometry of 1:1 (ligand:RNA). In contrast, TAR mutants maintaining the bulge region bind neomycin with a stoichiometry of 2:1 and neomycin dimers with a stoichiometry of 1:1, as observed with wildtype TAR RNA. Scatchard analysis was performed for the TAR RNA mutants lacking a bulge, revealing an association constant for neomycin in the low 10^7 M^{-1} range. This affinity of neomycin for TAR RNA mutants lacking a bulge region is higher than the previously reported micromolar affinity of neomycin for wildtype TAR RNA.

While neomycin shows increased affinity for TAR RNA mutants lacking the bulge region, when the bulge region is maintained, neomycin dimers show a distinctive advantage in binding compared to neomycin. This observation is relevant given that the bulge region of TAR RNA is required for Tat protein binding[66]. In addition, single base substitutions in the bulge region affect Tat protein binding [66]. The ability of neomycin dimers to recognize TAR RNA conformations in which the bulge region is maintained provides the conformational recognition necessary for inhibition of Tat protein binding. In addition, both the length and functionality of the neomycin dimer linker region have an effect on the affinities to the TAR RNA structures. Trends in affinity can be observed when comparing neomycin dimers with the same linker functionality but different lengths. Neomycin dimers DPA52, DPA54, and DPA56 have the same aliphatic linker functionality and differ only in their linker lengths of 7, 8, and 10 atoms, respectively. These three neomycin dimers show the same order of affinity to all TAR RNA structures with DPA52 having the highest affinity, followed by DPA56, and lastly DPA54. In addition, DPA58 and DPA60 also have the same linker functionality but differ in length by 4 atoms. Unlike the aliphatic linker neomycin dimers, DPA58 and DPA60 did not show the same trend in affinity for all TAR RNA structures. The affinity of DPA58 was higher for all the TAR RNA mutants, but DPA60 showed higher affinity for the wildtype TAR RNA. Based on linker length alone DPA60 showed selectivity for the wildtype TAR RNA over the TAR RNA mutants. These data demonstrate how linker length and functionality play a role in the recognition of TAR RNA structures. Generating multivalent amino sugars which display the same conformational recognition as target proteins but with increased affinities continues to highlight the potential for selective targeting of RNA structures by multivalent amino sugars.

Neomycin Dimer Binding Site on TAR RNA monitored by NMR Spectroscopy

Previous nuclear magnetic resonance (NMR) investigations of the wildtype TAR-neomycin interaction revealed that the intermolecular contacts are confined to the three nucleotide, U_3-bulge and the minor groove of the lower stem[67]. To better understand the differences in association constants and TAR's binding surface of neomycin dimers, we monitored the observable H1 and H3 imino proton resonances that are diagnostic for hydrogen-bonded guanine and uracil bases, respectively, which are protected from rapid exchange with the solvent (Figure 9).

In contrast to the U_3-bulge TAR-neomycin complex[67], the wildtype TAR-DPA51 complex adopts the slow exchange regime on the NMR timescale manifesting the higher affinity of neomycin dimers when compared to neomycin. While G21, U42 and G26 experience the most pronounced chemical shift differences ($\Delta\delta$) in the fast exchanging U_3-bulge TAR-neomycin complex, additional wildtype TAR imino resonances significantly change chemical shift as a function of increasing DPA51 concentration. Most notably, in good qualitative agreement with a 1:1 complex stoichiometry, at a molar ratio of 1.4:1.0 (DPA51:wildtype TAR) the imino resonances attributable to unbound TAR disappear. The DPA51-bound set of wildtype TAR imino resonances show the largest $\Delta\delta$ values (δ_{bound}- δ_{free}) for G28 and U38 (-0.068 and 0.092 ppm, respectively) followed by G21 and G26 (0.067 and -0.065 ppm, respectively) which are part of the previously identified neomycin binding interface (Figure 9). Based on the binding interface mapping, the higher affinity of DPA51 towards the wildtype TAR RNA can be attributed to extensive contacts involving the upper stem that are not limited to the G26-C39 base pair neighboring the tri-nucleotide bulge.

While replacement of the wild-type apical loop with a stable UUCG-tetraloop may not significantly affect the structural dynamics at the TAR bulge[68] local structural rearrangements of the upper stem involving the G28-C37, A27-U38 and even G26-C39 base pair can be detected by comparing imino chemical shifts of tetraloop- and wildtype TAR (Figure S5.1) variants ($\Delta\delta$ = -0.054 (G28), 0.089(U38) and 0.011(G26) [ppm]). The altered upper stem leads to reduced binding affinities (Table 3) which can also be observed when following the tetraloop TAR imino resonances as a function of increasing DPA51 concentrations (Figure S5.2). Based on similar or larger $\Delta\delta$ values measured for e.g. G21 and G26, (0.127 and -0.099 ppm, respectively) the neomycin binding site is unaffected in the tetraloop TAR variant. However, the extended interface involving the upper stem appears impaired as exemplified by U38's reduced. $\Delta\delta$ of merely 0.019 ppm thereby offering an explanation for the differential association constants of wildtype- and tetraloop TAR.

CONCLUSION

Neomycin dimers with variations in the linker region show different and selective binding to TAR RNA mutants that adopt different conformations. In addition, we show that differences in linker functionality of neomycin dimers induces different conformational changes in wildtype TAR RNA. The removal of the bulge region of TAR RNA (bulgeless and bulgeless tetraloop TAR RNA) eliminates the neomycin dimers' selective advantage over neomycin and in some cases neomycin shows higher affinity than the neomycin dimers to these bulgeless TAR RNA

mutants. Also removal of the bulge region resulted in greater increases in CD intensity from neomycin dimer DPA51 binding than did wildtype TAR RNA and TAR RNA mutants retaining the bulge region. When the bulge region is maintained neomycin dimers have a clear advantage in binding over neomycin alone. For the TAR RNA mutants maintaining the bulge region, changes to either the bulge or the loop regions both result in a decrease in neomycin dimer binding affinity when compared to wildtype TAR RNA. This may be attributed to neomycin dimer interactions with the upper stem of TAR RNA, as observed by NMR spectroscopy. NMR studies also corroborate 1:1 neomycin dimer:TAR RNA complex stoichiometry extrapolated from FID assay data. The observed differences in neomycin dimer binding for the different TAR RNA mutants shows that different linkers results in different recognition of the mutant TAR RNA structures providing insight to the ability to design future neomycin dimers to selectively recognize certain RNA structures.

Experimental section

TAR RNA Preparation

TAR RNA was purchased from Dharmacon, Inc. (Lafayette, CO) as stable 2`-ACE protected oligonucleotides, prior to use RNA was deprotected following the established 2`-ACE deprotection protocol. Deprotected RNA was suspended in 100 mM KCl, 10 mM SC, 0.5 mM EDTA, pH 6.8 and heated to 98 ^{o}C for 5 minutes, then cooled rapidly in ice bath for 15 minutes. This snap-cooling causes the RNA to adopt the kinetically favored hairpin rather than the thermodynamically favored duplexes.

To prepare TAR RNA samples for NMR studies, *in vitro* transcriptions with phage T7 polymerase from a linearized plasmid template were optimized and performed as described utilizing unlabeled NTPs (MP Biomedicals)[69, 70]. To resolve 3'-end heterogeneity, TAR transcripts incorporated *cis*-acting hammerhead ribozymes[71]. Self-cleaving of the phosphodiester bond occurs after the GUC (Figure 5)[72], resulting in a population of RNA transcripts with homogeneous 3'-ends. TAR transcripts were purified with a HiTrap Q (GE Healthcare), followed by a DNAPac PA200 column (Dionex). Purified RNA was annealed and equilibrated with NMR buffer (25 mM KCl, 10 mM sodium phosphate [pH 6.5], 500 µM EDTA (Ethylenediaminetetraacetic acid), 50 µM sodium azide, 9:1 H_2O:D_2O).

Circular Dichroism (CD) Spectroscopy

CD spectra samples (1.8 mL) of TAR RNA (4µM/strand or 2µM/strand) in 100 mM KCl, , 10 mM SC, 0.5 mM EDTA, pH 6.8. The CD spectra of TAR RNA samples in 1 cm path length quartz cuvettes were recorded as a function of wavelength from 325 nm to 200 nm at a scanning rate of 500 nm/min and a bandwidth of 1 nm at 20 ^{o}C. For CD spectra containing ligand, additions of concentrated ligand solution dissolved in 100 mM KCl, , 10 mM SC, 0.5 mM EDTA, pH 6.8 were added to the TAR RNA samples accounting for $\leq$ 1% (v/v). All CD spectra were recorded on a Jasco J-810 spectropolarimeter equipped with a thermoelectrically controlled cuvette holder. CD Spectra is represents the average of 10 scans.

UV Thermal Denaturation

UV thermal denaturation samples (1 mL) of TAR RNA (1 μM/strand) performed with DPA51 and neomycin were mixed with the ligand (1 or 2 molar equivalents) in 100 mM KCl, , 10 mM SC, 0.5 mM EDTA, pH 6.8 and incubated for 4 h at 4 ^{o}C before starting the experiment. The UV thermal denaturation spectra of the samples in 1 cm path length quartz cuvettes were recorded at 260 nm as a function of temperature (15-100 ^{o}C, heating rate: 0.3 ^{o}C/min). First derivative plots were used to determine the denaturation temperature (T_m). All UV spectra were recorded on a Cary 100 Bio UV/Vis spectrophotometer equipped with a thermoelectrically controlled 12-cell holder. Spectrophotometer stability and λ alignment were checked prior to initiation of each thermal denaturation experiment.

Ethidium Bromide Displacement Assay

A solution of ethidium bromide (5 μM, 1800 μL) was excited at 545 nm, and its fluorescence emission was monitored from 580 nm to 660 nm before and after the addition of TAR RNA. The concentration of TAR RNA was 200 nM/strand. A small fraction of ethidium bromide is bound (less than 20%) under these conditions. Additions of concentrated ligand aliquots dissolved in 100 mM KCl, 10 mM SC, 0.5 mM EDTA, pH 6.8 were sequentially added to the TAR RNA-EtBr complex accounting for $\leq$ 4% (v/v). Buffer conditions: 100 mM KCl, 10 mM SC, 0.5 mM EDTA, pH 6.8. Fluorescence spectra were measured on a Photon Technology International instrument (Lawrenceville, New Jersey, USA).

Nuclear Magnetic Resonance (NMR) Spectroscopy

All NMR spectra were recorded at 298K on a Bruker Avance III 850 MHz spectrometer equipped with a TCI-cryoprobe. NMR experiments were performed on samples of 500 μL volume containing 0.2-0.6 mM TAR RNA. Data were processed using NMRPipe[73] and analyzed using Sparky[74]. One-dimensional imino proton spectra were acquired using a jump-return echo sequence[75]. Imino resonance assignments were confirmed using water flip-back, WATERGATE 2D NOESY spectra (τ_{mix}=200ms)[76]. Separate solutions of ligands (ca. 10 mM) were dissolved in NMR buffer before performing NMR titrations. Binding of TAR and TAR variants to various ligands was monitored by changes in the imino 1D NMR spectrum in the absence and presence of an increasing concentration of ligand.

ACKNOWLEDGMENT
Financial support to this work was provided by National Institutes of Health (grants R15CA125724 and 1R41GM100607 to DPA) and by the National Science Foundation (MCB 0845512 to MH). We thank Dr. Nihar Ranjan (Clemson University) for his help with CD studies of TAR mutants with DPA 51.

Notes

[a]Laboratory of Medicinal Chemistry, Department of Chemistry, Clemson University, Clemson, South Carolina 29634, United States

[b]NUBAD, LLC, 900B West Faris Rd., Greenville, SC 29605
[c]Department of Biochemistry and Molecular Biology, Medical University of South Carolina, 70 President St., Charleston, SC 29425

* To whom correspondence should be addressed: Dev P Arya, 461 H.L. Hunter Chemistry Labs, Department of Chemistry, Clemson University, Clemson University, Clemson, South Carolina 29634; Phone: +1-864-656-1106; Fax: +1-864-656-6613; E-mail: dparya@clemson.edu.

[†]Electronic Supplementary Information (ESI) available: [Chemical structures of all compounds studied, CD spectroscopic characterization, UV thermal denaturation, ethidium bromide displacement assays and NMR characterizations].

References

1. B. Berkhout; K. T. Jeang *J. Virol. 1989***63,** 5501-5504.
2. K. A. Jones; B. M. Peterlin *Annu. Rev. Biochem. 1994***63,** 717-743.
3. D. E. Draper *Annu. Rev. Biochem. 1995***64,** 593-620.
4. C. A. Rosen; J. G. Sodroski; W. A. Haseltine *Cell 1985***41,** 813-823.
5. M. A. Muesing; D. H. Smith; D. J. Capon *Cell 1987***48,** 691-701.
6. F. Aboul-ela; J. Karn; G. Varani *J. Mol. Biol. 1995***253,** 313-332.
7. T. M. Rana; K. Jeang *Arch. Biochem. Biophys. 1999***365,** 175-185.
8. F. Aboul-ela; J. Karn; G. Varani *J. Mol. Biol. 1995***253,** 313-332.
9. H. M. Al-Hashimi; Y. Gosser; A. Gorin; W. Hu; A. Majumdar; D. J. Patel *J. Mol. Biol. 2002***315,** 95-102.
10. J. Hauber; B. R. Cullen *J. Virol. 1988***62,** 673-679.
11. S. Feng; E. C. Holland *Nature 1988***334,** 165-167.
12. D. I. Bryson; W. Zhang; P. M. McLendon; T. M. Reineke; W. L. Santos *ACS Chem. Biol. 2011***7,** 210-217.
13. J. R. Thomas; P. J. Hergenrother *Chem. Rev. 2008***108,** 1171-1224.
14. G. J. Zaman; P. J. Michiels; C. A. van Boeckel *Drug Discov. Today 2003***8,** 297-306.

15. A. P. Carter; W. M. Clemons; D. E. Brodersen; R. Morgan-Warren; B. T. Wimberly; V. Ramakrishnan *Nature 2000***407,** 340-348.
16. Y. Tor *Biochimie 2006***88,** 1045-1051.
17. D. E. Brodersen; W. M. J. Clemons; A. P. Carter; R. J. Morgan-Warren; B. T. Wimberly; V. Ramakrishnan *Cell 2000***103,** 1143-1154.
18. D. N. Wilson; J. M. Harms; K. H. Nierhaus; F. Schlunzen; P. Fucini *Biol Chem 2005***386,** 1239-1252.
19. T. Hermann *Curr. Opin. Struct. Biol. 2005***15,** 355-366.
20. K. L. Leach; S. M. Swaney; J. R. Colca; W. G. McDonald; J. R. Blinn; L. M. Thomasco; R. C. Gadwood; D. Shinabarger; L. Xiong; A. S. Mankin *Mol Cell 2007***26,** 393-402.
21. C. Bailly; P. Colson; C. Houssier; F. Hamy *Nucleic Acids Res. 1996***24,** 1460-1464.
22. L. Dassonneville; F. Hamy; P. Colson; C. Houssier; C. Bailly *Nucleic Acids Res. 1997***25,** 4487-4492.
23. K. E. Lind; Z. Du; K. Fujinaga; B. M. Peterlin; T. L. James *Chem. Biol. 2002***9,** 185-193.
24. J. Tao; A. D. Frankel *Proc. Natl. Acad. Sci. 1992***89,** 2723-2726.
25. S. Hwang; N. Tamilarasu; K. Ryan; I. Huq; S. Richter; W. C. Still; T. M. Rana *Proc. Natl. Acad. Sci. 1999***96,** 12997-13002.
26. Z. Athanassiou; K. Patora; R. L. A. Dias; K. Moehle; J. A. Robinson; G. Varani *Biochemistry (N. Y.) 2007***46,** 741-751.
27. H. Mei; D. P. Mack; A. A. Galan; N. S. Halim; A. Heldsinger; J. A. Loo; D. W. Moreland; K. A. Sannes-Lowery; L. Sharmeen; H. N. Truong; A. W. Czarnik *Bioorg. Med. Chem. 1997***5,** 1173-1184.
28. S. Kumar; P. Kellish; W. E. Robinson; D. Wang; D. H. Appella; D. P. Arya *Biochemisry 2012***51,** 2331-2347.
29. D. Raghunathan; V. M. Sánchez-Pedregal; J. Junker; C. Schwiegk; M. Kalesse; A. Kirschning; T. Carlomagno *Nucleic Acids Res. 2006***34,** 3599-3608.
30. S. Wang; P. W. Huber; M. Cui; A. W. Czarnik; H. -. Mei *Biochemistry (N. Y.) 1998***37,** 5549-5557.
31. I. Charles; H. Xi; D. P. Arya *Bioconjug. Chem. 2007***18,** 160-169.
32. N. N. Shaw; D. P. Arya *Biochimie 2008***90,** 1026-1039.
33. N. N. Shaw; H. Xi; D. P. Arya *Bioorg. Med. Chem. Lett. 2008***18,** 4142-4145.
34. H. Xi; D. Gray; S. Kumar; D. P. Arya *FEBS Lett. 2009***583,** 2269-2275.
35. D. P. Arya *Acc. Chem. Res. 2011***44,** 134-146.
36. H. Xi; E. Davis; N. Ranjan; L. Xue; D. Hyde-Volpe; D. P. Arya *Biochemistry 2011***50,** 9088-9113.
37. L. Xue; N. Ranjan; D. P. Arya *Biochemisry 2011***50,** 2838-2849.
38. N. Ranjan; K. F. Andreasen; S. Kumar; D. Hyde-Volpe; D. P. Arya *Biochemistry 2010***49,** 9891-9903.
39. B. Willis; D. P. Arya *Biochemistry 2010***49,** 452-469.
40. H. Xi; S. Kumar; L. Dosen-Micovic; D. P. Arya *Biochimie 2010***92,** 514-529.
41. L. Xue; H. Xi; S. Kumar; D. Gray; E. Davis; P. Hamilton; M. Skriba; D. P. Arya *Biochemistry 2010***49,** 5540-5552.
42. B. Willis; D. P. Arya *Bioorg. Med. Chem. Lett. 2009***19,** 4974-4979.
43. B. Willis; D. P. Arya *Curr. Org. Chem. 2006***10,** 663-673.
44. B. Willis; D. P. Arya *Biochemistry (N. Y.) 2006***45,** 10217-10232.
45. B. Willis; D. P. Arya *Adv. Carbohydr. Chem. Biochem. 2006***60,** 251-302.

46. D. P. Arya *Top. Curr. Chem. 2005***253,** 149-178.
47. H. Xi; D. P. Arya *Curr Med Chem Anticancer Agents 2005***5,** 327-338.
48. D. P. Arya; L. Xue; B. Willis *J. Am. Chem. Soc. 2003***125,** 10148-10149.
49. D. P. Arya; L. Micovic; I. Charles; R. L. C. Jr.; B. Willis; L. Xue *J. Am. Chem. Soc. 2003***125,** 3733-3744.
50. D. P. Arya; B. Willis *J. Am. Chem. Soc. 2003***125,** 12398-12399.
51. D. P. Arya; L. Xue; P. Tennant *J. Am. Chem. Soc. 2003***125,** 8070-8071.
52. L. Xue; I. Charles; D. P. Arya *Chem. Commun. 2002***1,** 70-71.
53. P. L. Hamilton; D. P. Arya *Nat. Prod. Rep. 2012***29,** 134-143.
54. D. P. Arya; R. L. Coffee Jr. *Bioorg. Med. Chem. Lett. 2000***10,** 1897-1899.
55. D. P. Arya; R. L. C. Jr.; B. Willis; A. I. Abramovitch *J. Am. Chem. Soc. 2001***123,** 5385-5395.
56. D. P. Arya; R. L. C. Jr.; I. Charles *J. Am. Chem. Soc. 2001***123,** 11093-11094.
57. H. Mei; A. A. Galan; N. S. Halim; D. P. Mack; D. W. Moreland; K. B. Sanders; H. N. Truong; A. W. Czarnik *Bioorg. Med. Chem. Lett. 1995***5,** 2755-2760.
58. R. Pang; C. Zhang; D. Yuan; M. Yang *Bioorg. Med. Chem. 2008***16,** 8178-8186.
59. B. Davis; M. Afshar; G. Varani; A. I. H. Murchie; J. Karn; G. Lentzen; M. Drysdale; J. Bower; A. J. Potter; I. D. Starkey; T. Swarbrick; F. Aboul-ela *J. Mol. Biol. 2004***336,** 343-356.
60. A. I. Murchie; B. Davis; C. Isel; M. Afshar; M. J. Drysdale; J. Bower; A. J. Potter; I. D. Starkey; T. M. Swarbrick; S. Mirza; C. D. Prescott; P. Vaglio; F. Aboul-ela; J. Karn *J. Mol. Biol. 2004***336,** 625-638.
61. N. Ranjan; S. Kumar; D. Watkins; D. Wang; D. H. Appella; D. P. Arya *Bioorg Med Chem Lett 2013***20,** 5689-5693.
62. H. Suryawanshi; H. Sabharwal ; S. Maiti *J. Phys. Chem. B 2010***114,** 11155-11163.
63. S. Wang; P. W. Huber; M. Cui; A. W. Czarnik; H. Mei *Biochemistry (N. Y.) 1998***37,** 5549-5557.
64. E. A. Dethoff; A. L. Hansen; C. Musselman; E. D. Watt; I. Andricioaei; H. M. Al-Hashimi *Biophys. J. 2008***95,** 3906.
65. D. L. Boger; B. E. Fink; S. R. Brunette; W. C. Tse; M. P. Hendrick *J. Am. Chem. Soc. 2001***123,** 5878-5891.
66. S. Roy; U. Delling; C. H. Chen; C. A. Rosen; N. Sonenberg *Genes and Development 1990***4,** 1365-1373.
67. C. Faber *J Biol Chem 2000***275,** 20660--20666.
68. E. A. Dethoff *Biophys J 2008***95,** 3906--0915.
69. L. G. Scott; M. Hennig *Methods Mol. Biol. 2008***452,** 29--61.
70. B. M. Roth RNA Structure Determination by NMR: Combining Labeling and Pulse Techniques. In *Biomolecular NMR Spectroscopy;* Dingey, A. and Pascal S.M., Ed.; IOS Press: 2011; pp 205-228.
71. S. R. Price; N. Ito; C. Oubridge; J. M. Avis; K. Nagai *J Mol Biol 1995***249,** 398--408.
72. E. Wyszko; J. P. Fuerste; M. Barciszewska; M. Syzmanski; R. Adamiak; V. A. Erdmann; J. Barciszewski *J Biochem 1999***126,** 326--332.
73. F. Delaglio; S. Grzesiak; G. W. Vuister; G. Zhu; J. Pfiefer *J Biomol NMR 1995***6,** 277--293.
74. Goddard T. D.; Kneller D. G. .
75. V. Sklenar; B. R. Brooks; G. Zon; A. Bax *FEBS Lett 1987***216,** 249--252.
76. G. Lippens; C. Dhalluin; J. M. Wieruszeski *J Biomol NMR 1995***5,** 327--331.

Figures:

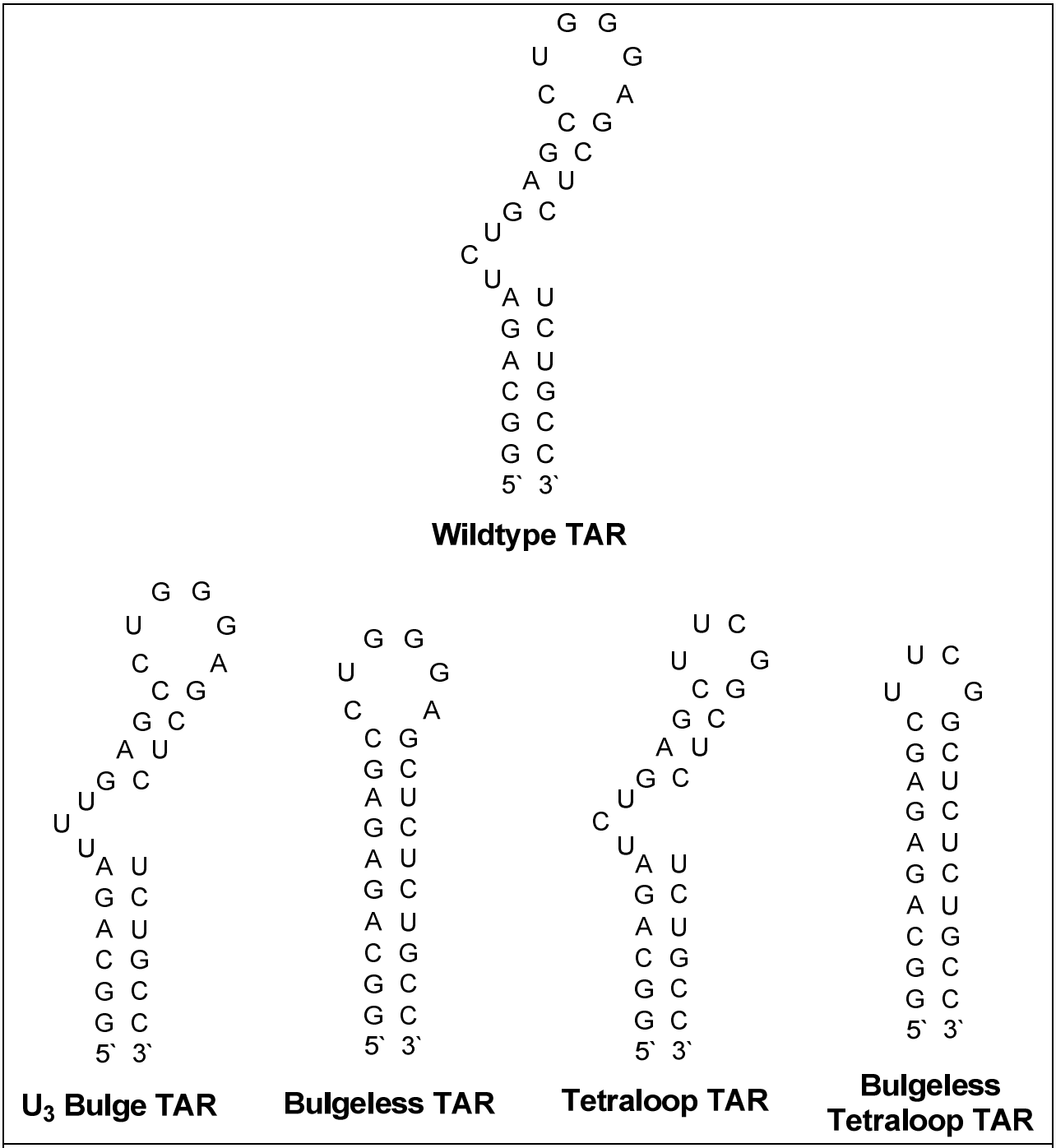

Figure 1. *Sequence and secondary structure of wildtype TAR RNA and TAR RNA mutants.*

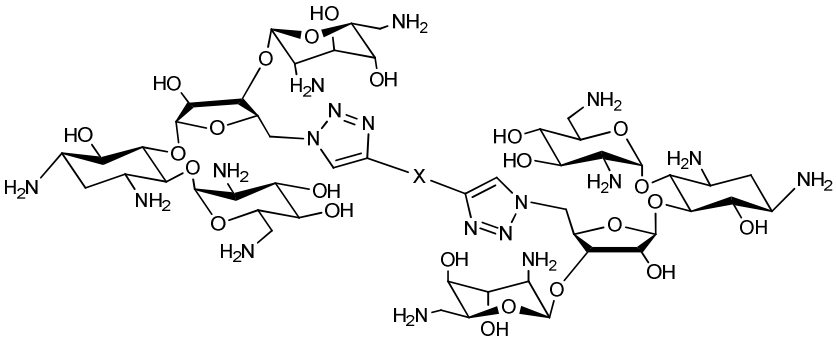

	—X—
DPA51	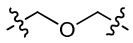
DPA52	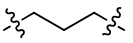
DPA53	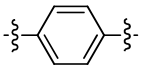
DPA54	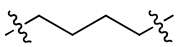
DPA55	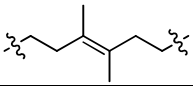
DPA56	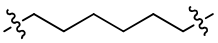
DPA58	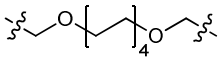
DPA60	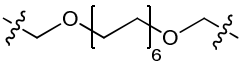
DPA65	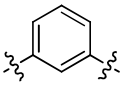

Figure 2. *Structure of trizole-linked neomycin dimers synthesized using "click chemistry" where X represents the various functionalities in the linker region of the neomycin dimers.*

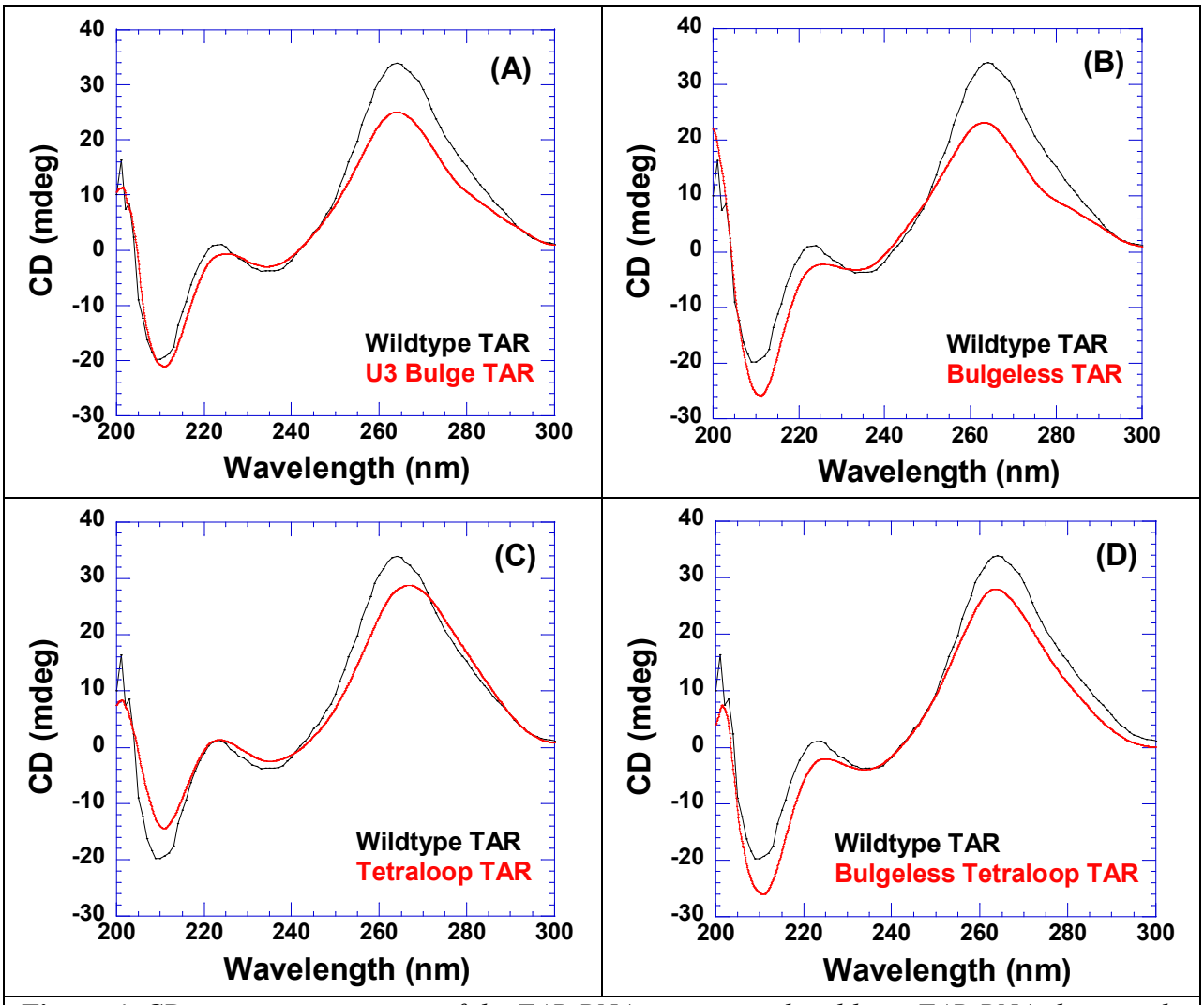

Figure 4. *CD spectra comparison of the TAR RNA mutants with wildtype TAR RNA showing the conformational differences between mutant TAR RNA and wildtype TAR RNA. CD spectra of wildtype TAR RNA with the U3 bulge mutant (A), bulgeless mutant (B), tetraloop mutant (C), and bulgeless tetraloop mutant (D). Buffer conditions: 100 mM KCl, 10 mM SC, 0.5 mM EDTA, pH 6.8. [TAR RNA] = 4 μM/strand.*

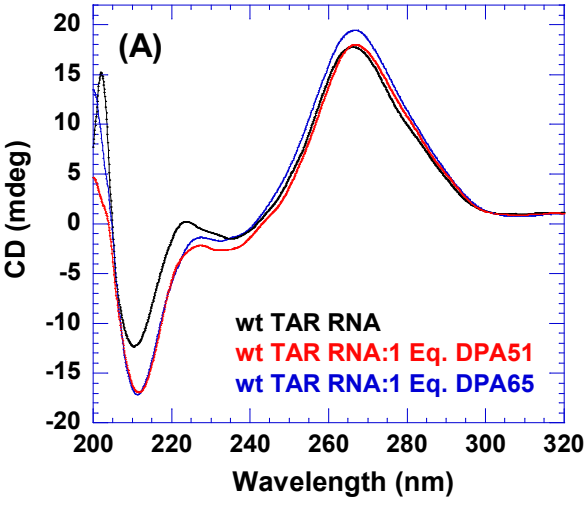

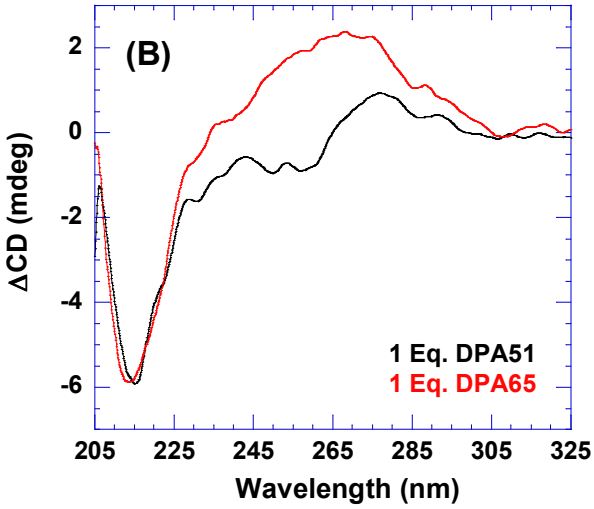

Figure 3. *CD spectra comparison of wildtype TAR RNA with 1 molar equivalent DPA51 and DPA65 (A). Plot showing the change in CD induced by the binding of 1 molar equivalent DPA51 and DPA65 (B). Buffer conditions: 100 mM KCl, 10 mM SC, 0.5 mM EDTA, pH 6.8. [TAR RNA] = 2μM/strand.*

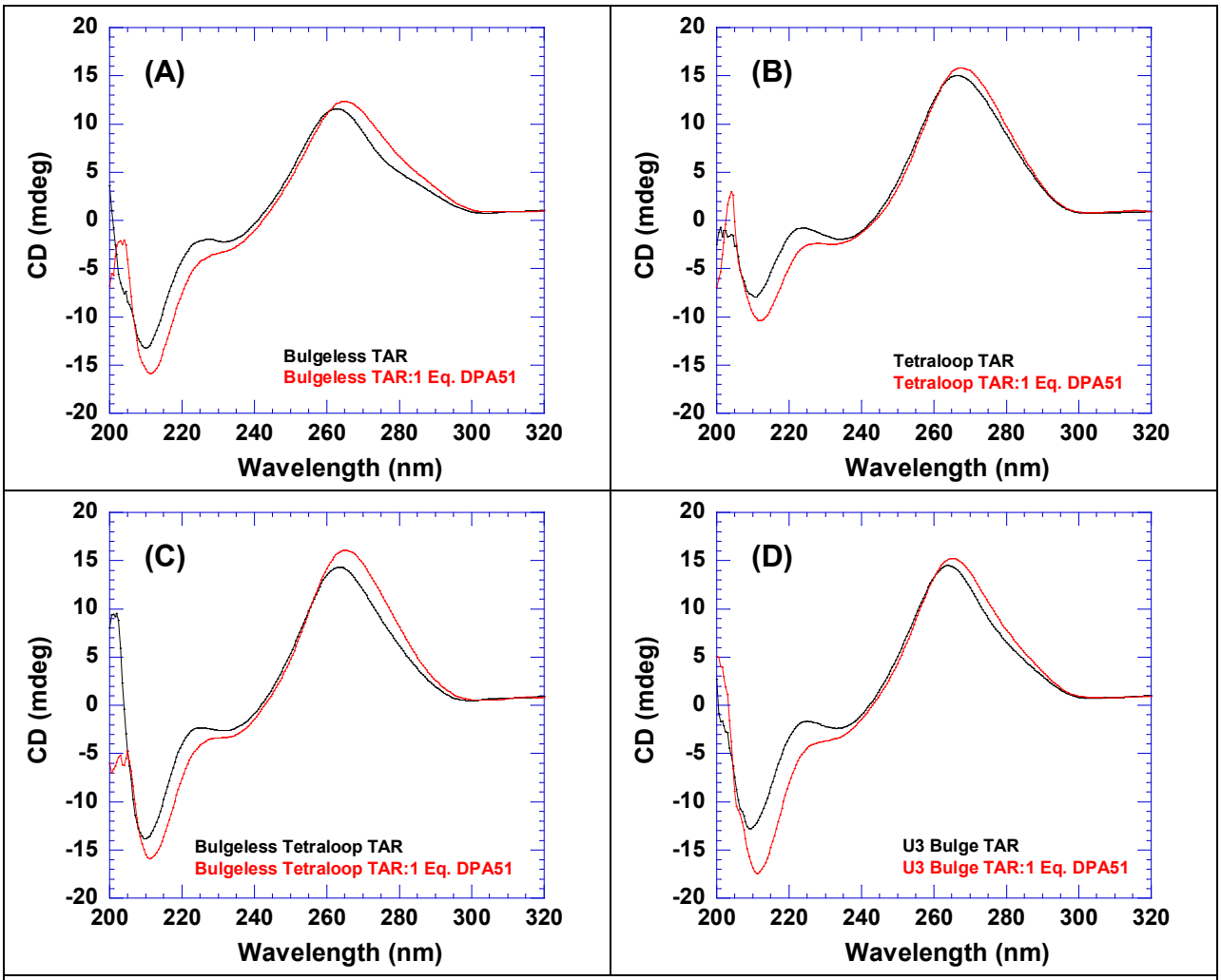

Figure 5. *CD spectra comparison of the TAR RNA mutants with 1 molar equivalent DPA51. CD spectra before and after addition of 1 molar equivalent DPA51 for the bulgeless (A), tetraloop (B), bulgeless tetraloop (C), and U3 bulge (D) TAR RNA mutants. Buffer conditions: 100 mM KCl, 10 mM SC, 0.5 mM EDTA, pH 6.8. [TAR RNA] = 2μM/strand.*

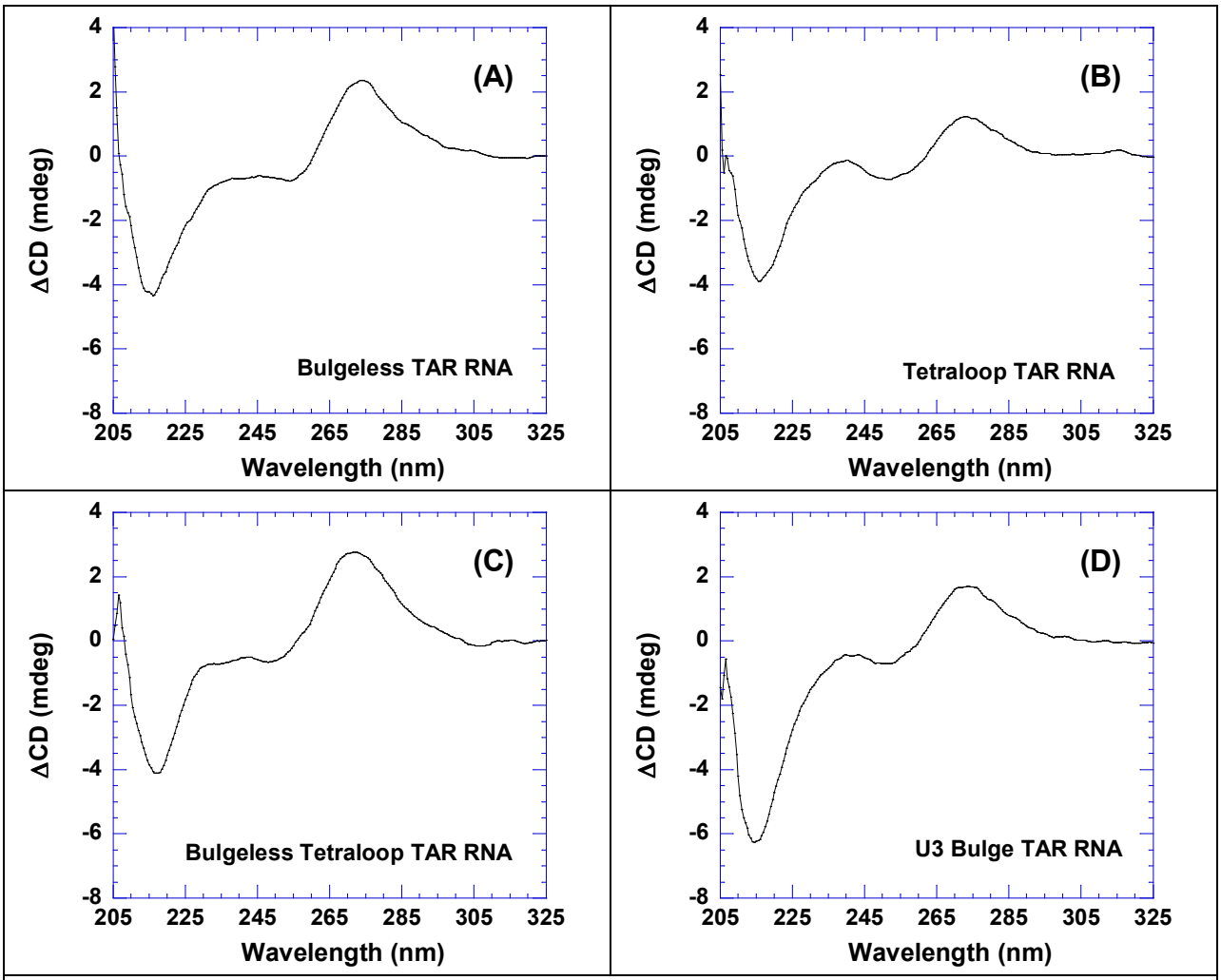

Figure 6. *Plots showing the change in CD (ΔCD) induced by the of 1 molar equivalent DPA51 for the bulgeless (A), tetraloop (B), bulgeless tetraloop (C), and U3 bulge (D) TAR RNA mutants. Buffer conditions: 100 mM KCl, 10 mM SC, 0.5 mM EDTA, pH 6.8. [TAR RNA] = 2μM/strand.*

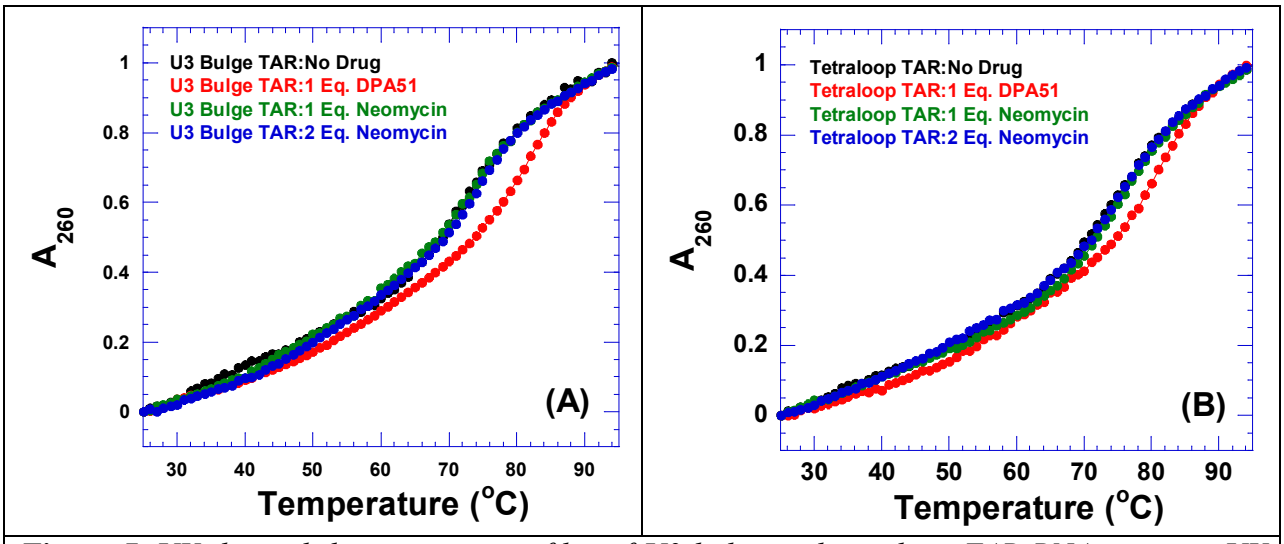

Figure 7. *UV thermal denaturation profiles of U3 bulge and tetraloop TAR RNA mutants. UV thermal denaturation profiles shown for U3 bulge TAR RNA mutant (A) and tetraloop TAR RNA mutant (B) without ligand, 1 molar equivalent DPA51, 1 molar equivalent neomycin, and 2 molar equivalents neomycin. Buffer conditions: 100 mM KCl, 10 mM SC, 0.5 mM EDTA, pH 6.8. [TAR RNA] = 1μM/strand. The heating rate was 0.3 °C/minute.*

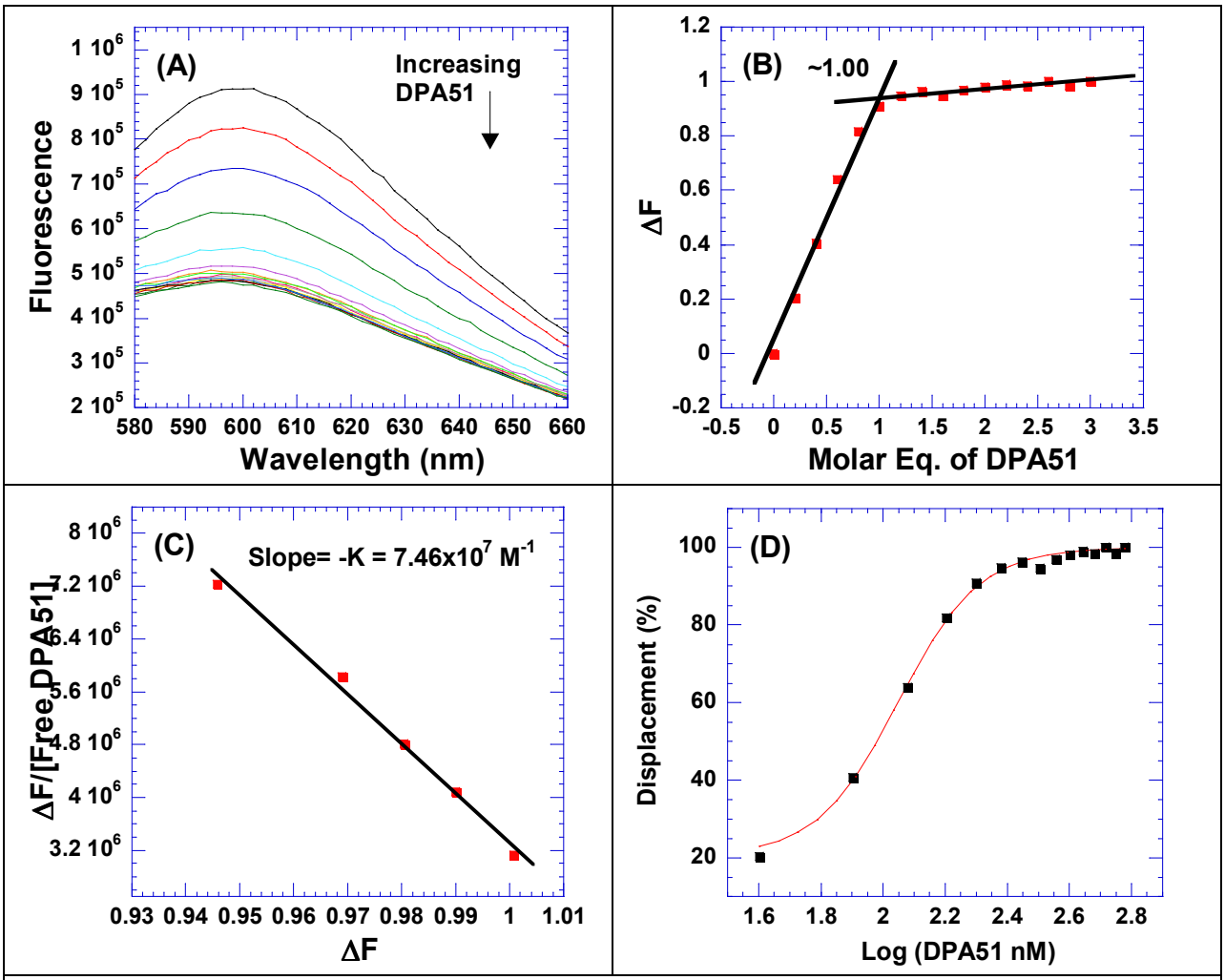

Figure 8. *FID titration of DPA51 with the bulgeless TAR RNA mutant. Raw fluorescence emission spectra in the presence of increasing concentration of DPA51 (A). Plot between normalized fluorescence intensity (at 610 nm) of the bulgeless TAR RNA mutant-EtBr complex as a function of concentration of DPA51 results in a saturating binding plot (B). Scatchard plot analysis of DPA51 with the bulgeless TAR RNA mutant (C). The plot for fraction of ethidium bromide displaced from the bulgeless TAR RNA mutant versus the log of DPA51 concentration, the data, shown with a sigmoidal fit was used to determine the IC_{50} value (D). Buffer conditions: 100 mM KCl, 10 mM SC, 0.5 mM EDTA, pH 6.8. Bulgeless TAR RNA mutant = 200 nM/strand. [EtBr] = 5 μM.*

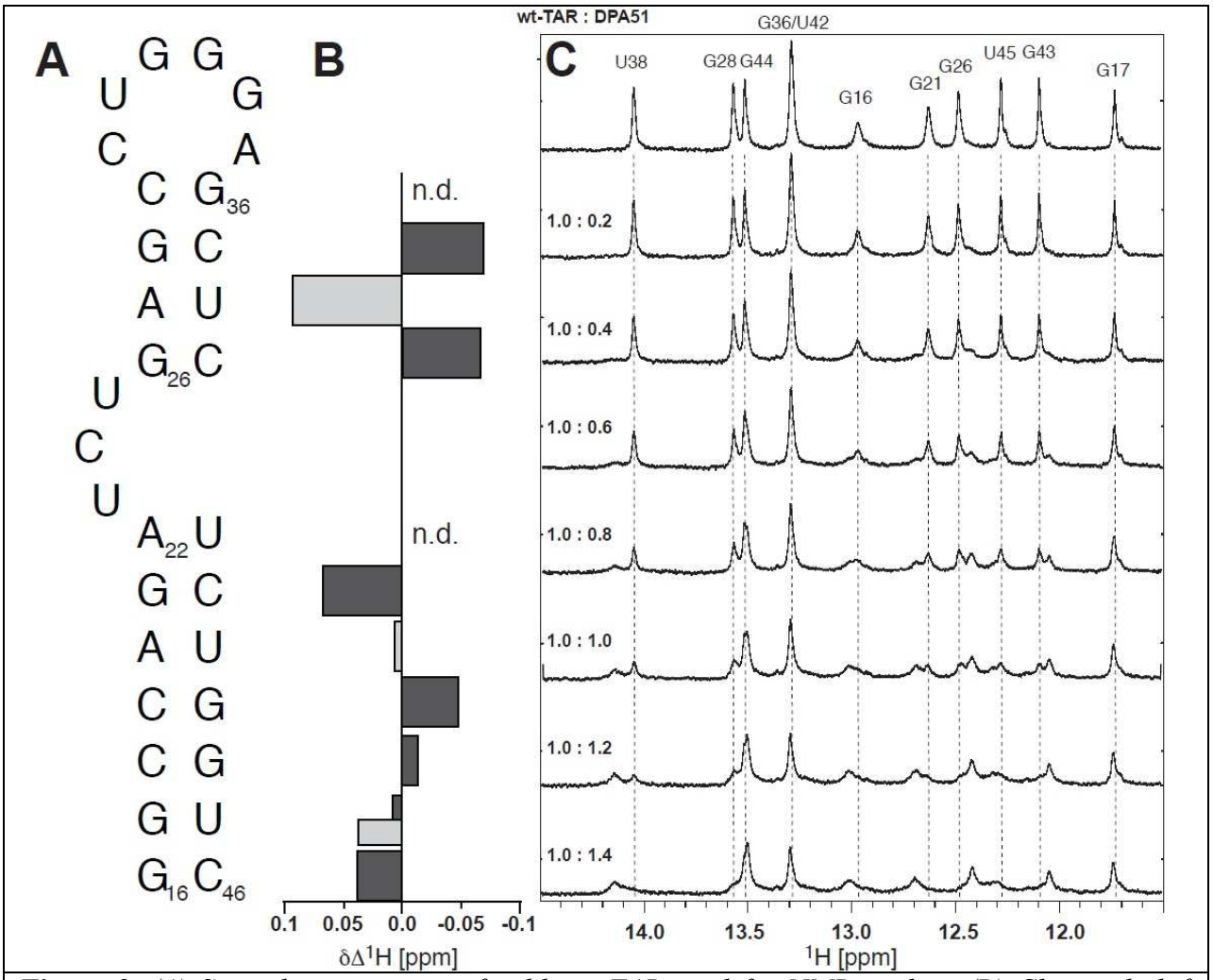

Figure 9. *(A) Secondary structure of wildtype TAR used for NMR studies. (B) Chemical shift changes ($\Delta\delta=\delta_{bound} - \delta_{free}$ [ppm]) of GH1 (dark gray bars) and UH3 (light gray bars), respectively, observed for the wildtype TAR-DPA51 complex. Overlapped- or imino resonances broadened beyond detection are labeled n.d. (not determined) (C) Imino regions of 1D ^{1}H-jump-return echo experiments of wildtype TAR with increasing amounts of DPA51. Data were collected on a wildtype TAR sample containing ca. 0.25 mM RNA in 500 µL volume of NMR buffer. Spectra were recorded at 298K on a Bruker Avance III 850 MHz spectrometer. Dashed black lines follow assigned imino proton resonances at various molar ratios of wildtype TAR:DPA51.*

Tables:

Table 1. Effect of Ligand on the Thermal Denaturation of TAR RNA

		ΔT_m (°C)		
TAR RNA	T_m (°C)	1 Eq. DPA51	1 Eq. neomycin	2 Eq. neomycin
Wildtype	68.9	10.2	0.2	0.5
U3 Bulge	73	8.5	0.0	1.0
Tetraloop	74	6.0	1.0	1.0
Bulgeless	92	5.0	1	-
Bulgeless Tetraloop	95	>5	0.0	-

T_m values shown for wildtype TAR RNA and TAR RNA mutants, and ΔT_m values shown with 1 molar equivalent DPA51, 1 molar equivalent neomycin, and 2 molar equivalents neomycin. Buffer conditions: 100 mM KCl, 10 mM SC, 0.5 mM EDTA, pH 6.8. [TAR RNA] = 1μM/strand. The heating rate was 0.3 °C/minute.

Table 2. IC_{50} Values of TAR RNA with Neomycin Dimers

Ligand	Linker Length	IC_{50} (nM)				
		Wildtype	Bulgeless	Tetraloop	Bulgeless Tetraloop	U_3 Bulge
DPA51	7	112	112	156	122	186
DPA52	7	118	134	190	146	224
DPA65	7	110	130	180	142	244
DPA53	8	150	-	-	-	-
DPA54	8	144	160	278	216	278
DPA55	10	146	142	210	162	338
DPA56	10	126	146	214	150	256
DPA58	16	156	108	188	106	234
DPA60	20	144	144	300	158	326
Neo	N/A	378	150	684	192	-

Table representing the IC_{50} values from an ethidium bromide displacement assay of the neomycin dimers and neomycin with wildtype and mutant TAR RNAs. Buffer conditions: 100 mM KCl, 10 mM SC, 0.5 mM EDTA, pH 6.8. [TAR RNA] = 200 nM/strand. [EtBr] = 5 μM.

Table 3. Binding Constants of Neomycin Dimers with TAR RNA

Ligand	Linker Length	K (M^{-1})				
		Wildtype	Bulgeless	Tetraloop	Bulgeless Tetraloop	U_3 Bulge
DPA51	7	$1.2x10^8$	$7.5x10^7$	$2.7x10^7$	$2.3x10^8$	$1.6x10^7$
DPA52	7	$7.1x10^7$	$8.9x10^7$	$1.4x10^7$	$7.5x10^7$	$6.9x10^6$
DPA65	7	$1.4x10^8$	$1.0x10^8$	$1.3x10^7$	$6.9x10^7$	-
DPA53	8	$1.5x10^8$	-	-	-	-
DPA54	8	$2.6x10^7$	$2.2x10^7$	-	$1.2x10^7$	$2.1x10^6$
DPA55	10	$1.1x10^7$	$3.6x10^7$	$3.5x10^6$	$2.8x10^7$	$2.6x10^6$
DPA56	10	$6.6x10^7$	$6.3x10^7$	$5.0x10^6$	$5.9x10^7$	$3.8x10^6$
DPA58	16	$7.6x10^6$	$6.8x10^7$	$1.4x10^7$	$7.2x10^7$	$4.8x10^6$
DPA60	20	$2.5x10^7$	$4.4x10^7$	$2.0x10^6$	$2.7x10^7$	$1.5x10^6$
Neo	N/A	-	$3.0x10^7$	-	$1.6x10^7$	-

Table representing the binding constants derived from Scatchard analysis from the ethidium bromide displacement assay using the neomycin dimers and neomycin with wildtype and mutant TAR RNA. Buffer conditions: 100 mM KCl, 10 mM SC, 0.5 mM EDTA, pH 6.8. [TAR RNA] = 200 nM/strand. [EtBr] = 5 μM.